RESEARCH ARTICLE   OPEN ACCESS

Closed Loop Control of Single Phase Bridgeless Resonant AC-DC Converter

Monica S*, Dr. P Usha **

*(Department of Electrical & Electronics Engineering, Dayananda sagar college of engineering, Bangalore-560078
** (HoD, Department of Electrical & Electronics Engineering, Dayananda sagar college of engineering, Bangalore-560078

ABSTRACT
This paper presents a single phase bridgeless resonant ac-dc converter. By using a bidirectional switch, we expel a full-bridge diode rectifier from the grid side of the proposed converter and in this way it decreases the number of components used and reduces the conduction loss in the primary side. To adjust the converter to 1-kW power applications with a bidirectional switch, we utilized a series resonant circuit in the secondary side. The series resonant circuit gives zero-current switching turn-off at the output diode, and consequently reduces the reverse recovery loss. In following, the principle of operation of the proposed converter are explained, the proposed converter operates in continuous conduction mode and achieves high power factor of 0.9. Simulation results of open loop and closed loop systems are developed using MATLAB/Simulink. The simulation results of proposed converter are compared with the theoretical results.
*Keywords-*ac-dc power conversion, bidirectional switch, bridgeless converter, continuous conduction mode.

I. INTRODUCTION

Power factor correction (PFC) ac-dc converters are broadly utilized in grid connected power supply systems. These PFC ac-dc converters must meet standards and harmonic regulation requirements such as IEC 61000-3-2 and IEEE 519; and should accomplish high power density at low system cost. In addition it must accomplish high conversion efficiency with low input-current harmonics, high PFC capability, and good voltage regulation [1].

Development of efficient PFC ac-dc converters has been the subject of considerable research. Single-stage PFC ac-dc converters are considered attractive because they have a less number of components, low cost, and high conversion efficiency [2-6]. However, they suffer low power factor (PF) and they require a large dc link electrolytic capacitor and an inductor, which increases the size and cost of the converter. As another solution, single power conversion PFC ac-dc converters have been introduced [7-9]; they do not require a large inductor or large dc-link electrolytic capacitor. They can achieve high PF under grid voltage variations or load. However, these single power-conversion PFC ac-dc converters use bridge diodes on the input side of the rectifier, which causes high conduction losses and overheating.

Bridgeless converters have been introduced [10-17] to overcome the problems of conventional converters. To start with, bridgeless PFC boost rectifiers were proposed [10, 11]. Compared to the conventional PFC boost rectifiers, these bridgeless PFC boost rectifiers increase the efficiency of the front-end PFC stage by eliminating the diodes and their forward-voltage drop. Furthermore, PFC boost rectifier output voltage is always higher than the peak of grid voltage, and therefore it cannot be used for low-voltage applications. Bridgeless single-stage ac/dc converters have been propose to produce adjustable output voltages [12-16]. They help to reduce the number of components, but these are still large. Bridgeless flyback rectifier is presented to minimize the required number of components [17]. It does not utilize bridge diodes, so it does not suffer from diode conduction loss. However, requires auxillary circuits for proper operation. Also, the fly-back structure is usually restricted to low-power applications since it requires large magnetic components for high-power applications. Moreover, in the flyback structure the transformer

usage is poor and large transformer core is required to maintain the expected power level.

This paper presents a single phase bridgeless resonant ac-dc converter. It is low in cost, simple in structure and low in conduction loss since it uses a single bidirectional switch instead of input bridge diodes. To obtain high power capability with single bidirectional switch, the proposed single phase bridgeless resonant converter uses a series resonant circuit on the secondary side. The series resonant circuit achieves zero-current switching (ZCS) turnoff at the output diode and therefore reduces the reverse-recovery loss.

To achieve medium-high power capacity with appropriate size of the transformer, it operates in continuous conduction mode (CCM) when the instantaneous power level is high. The design guidelines of the proposed converter are presented and simulation results are obtained.

II. TOPOLOGY AND OPERATING PRINCIPLE

Fig. 1 shows the circuit diagram of the proposed single phase bridgeless resonant ac-dc converter. The bidirectional switch is used to transfer energy to the secondary side without rectifying the ac grid voltage. During the positive half cycle of the input voltage vg, the main switch S1 is turned on according to the duty-ratio. During the negative half-cycle of vg, switch S2 is turned on and acts as the main switch. S1 and S2 operates complementary to one another. When the bidirectional switch is turned on, the energy in the primary side is transferred to the secondary side through the series-resonant circuit. When the bidirectional switch is turned off, the energy which is stored in Lm is transferred to the secondary side. This characteristic enables the proposed converter to process high power by using a single bidirectional switch.
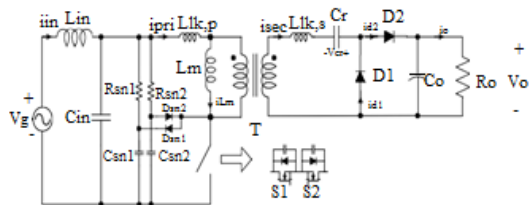

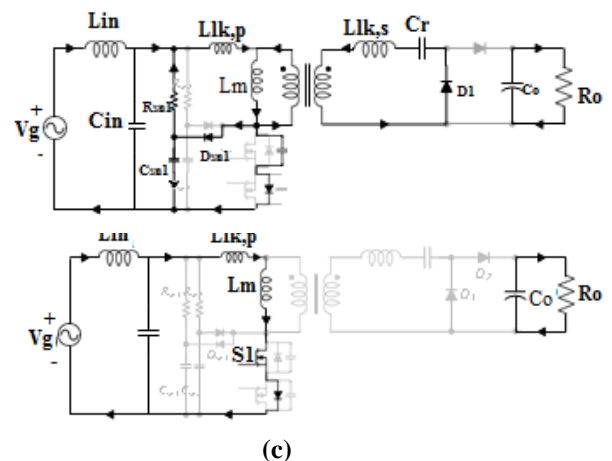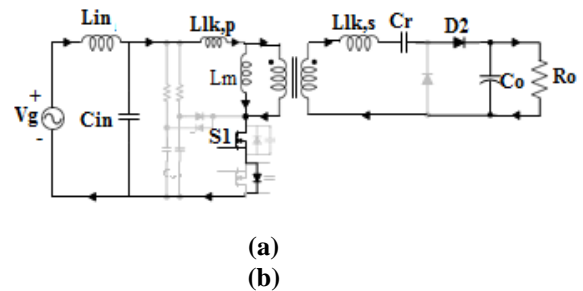**Fig. 1. Circuit diagram of bridgeless resonant ac-dc converter.**

The proposed converter is designed to operate in DCM when the instantaneous power level is low, and in CCM when the instantaneous

power level is high. The proposed converter requires less peak current and achieves high efficiency when it operates in CCM than when it operates in DCM. As the magnetizing inductance Lm increases, the CCM region in a single grid period widens, and thereby it increases the power conversion efficiency. However, large Lm requires large transformer size, so Lm must be selected cautiously to optimize the trade-off between efficiency and transformer size. During CCM steady-state operation, according to the switch and diode states Ts is divided into four operating modes. The equivalent circuit of each operating modes are shown in Fig. 2.

To analyze the operation of the proposed converter, several assumptions are made:

1) The grid voltage vg is constant because the the grid frequency fg is much lesser than the switching frequency fs;

2) The output capacitor Co is large that the output voltage Vo is assumed to have no ripple voltage;

3) The transformer is ideal with the primary leakage inductance Llk,p the magnetizing inductance Lm, and the secondary leakage inductance Llk,s;

4) The switch S1 is modulated with duty ratio D, and the switch S2 acts complementary to S1.

2.1 CCM Operation

(a)
(b)

(c)
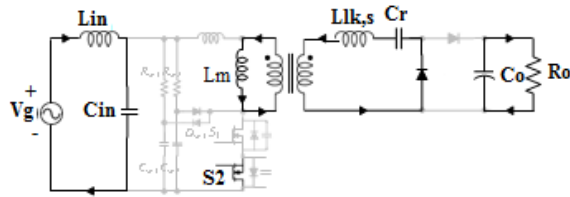
(d)
Fig. 2. Equivalent circuit of bridgeless resonant ac-dc converter when operates in CCM.
(a) Mode 1. (b) Mode 2. (c) Mode 3. (d) Mode 4.

Mode 1 [t_0, t_1]: At time t_0, $S_1$is turned on andi_{sec} starts to resonate due to $L_{lk,s}$and C_r and it is directly transfered to the load through D_2.For the simplicity, we ignored input filter effect and considered V_{cin} as V_g; During $T_s V_g$ is considered to be constant . Also, we assume $L_m \gg L_{lk,p}$ for the brevity. Then, i_{Lm} increases linearly as

$$\frac{di_{Lm}(t)}{dt} = \frac{V_g}{Lm} \quad .(1)$$

During this interval, the input power is transferred to the output stage of the transformer and it charges the magnetic inductor Lm.

since, $L_m \gg L_{lk,p}$, the transformer secondary side voltage can be expressed as nvg. The state equation of the circuit can be written as

$$L_{lk,s}\frac{di_{sec}(t)}{dt} = \text{nvg- Vo}+v_{cr}(t), \quad (2)$$

$$i_{sec}(t)= -C_r\frac{dv_{cr}(t)}{dt} \quad (3)$$

with isec(to) = 0, where vcr is the voltage across Cr. Solving (2) and (3) yields

$$i_{sec}(t)=\frac{nV_g-(Vo-V_{cr}(to))}{Zr}\sin[\omega_r(t-to)] \quad (4)$$

where thecharacteristic impedance Zr and the resonant angular frequency wr are given by

$$Zr=\sqrt{\frac{Llk,s}{Cr}}, \quad w_r = \frac{1}{\sqrt{L_{lk,s}C_r}}$$

At the same time, the input power charges magnetic inductor Lm and iLm is increased linearly as

$$i_{Lm}(t) =i_{Lm}(t_o) + \frac{V_g}{L_m}(t\text{-}t_0) \quad (5)$$

where iLm(to) is the initial value of iLm(t).

Mode 2 [t_1, t_2]: At time t1, the resonance between Cr and Llk,s terminates and isec becomes zero. The diode D2 is turned off withzero current (zcs) andtherefore reverse-recovery loss does not occur. The input power charges the magnetic inductor Lm and iLm increases linearly as

$$i_{Lm}(t) =i_{Lm}(t_o) + \frac{V_g}{L_m}(t\text{-}t_0) \quad (6)$$

$$i_{sec}(t)=0 \quad (7)$$

Mode 3 [t_2, t_3]: At time t2, S1 is turned off and magnetic inductor current iLm is transferred to the secondary side. A high voltage spike occurs at the switch because turned-off of the switch interrupts the current flowing through the transformer leakage inductance.

Here, theRCD snubber circuit absorbs the primary leakage inductorcurrent by turning on the snubber diode when vds exceeds vg + vcr/n.

Mode 4 [t_3, t_4]: At t2isec already begins to resonate due to Lm and Cr. iLm(t2) is reflected on the initial value of the secondary side

Then, the state equation of isec can be written as

$$i_{sec}(t)=-\frac{v_g}{nL_m}DT_s+\frac{V_{cr}}{n^2L_m}(t-t_2) \quad (8)$$

III. DESIGN GUIDELINES

3.1 Determining resonant capacitance:
To guarantee zero current switching(zcs) turn-off at output diode D2, half of the resonant period must be lesser than the minimum turn-ontime of the switch or

$$\pi\sqrt{L_{lk,s}C_r} < D_{min}T_s \quad (9)$$

The minimum duty ratio D_{min} is given as

$$D_{min} = 1\text{-}\frac{\sqrt{2}nV_{grms}}{Vo}, \quad (10)$$

From which

$$C_r < \frac{T_s^2}{\pi^2 L_{lk,s}}\left(1 - \frac{\sqrt{2}nV_{grms}}{Vo}\right)(12)$$

3.2 Determining magnetizing inductance:
The proposed converter operates in CCM when vg ≥ vg,crit, and in DCM otherwise. The boundary between CCM and DCM is determined by Lm. Increase in Lm widens the CCM region, and increases the efficiency, but it increases the size and cost of the converter. Thus, magnetizinginductance Lm must be chosen appropriately.

3.2 Determining output capacitance:
To satisfy the output voltage ripple, we select the output capacitor as

$$C_o \geq \frac{P_0}{2\pi f_g V_0 \Delta V_0} \quad (13)$$

where ΔVo-output voltage ripple.

3.3 Selecting transformer turns ratio:
The transformer turns ratio can be selected from the voltage gain of the proposed converter.

$$n \leq \frac{V_o}{\sqrt{2}V_{grms}}(14)$$

IV. SIMULATION RESULTS:

To evaluate the performance of the proposed converter, simulation was performed using MATLAB/SIMULINK with grid voltageVg=120—240 V; output voltage Vo = 360 V; and output power Po = 1 kW. To satisfy Zero current switching (ZCS) turn-off at D2 over the entire grid period, resonant capacitance (Cr) is set to 4.4 μF. Considering the size and cost of the

converter, magnetizing inductance (Lm) was set to 300 µH.

The open loop simulation is as shown in fig. 3.1. The selected specific components (Table I) were the same as in the simulation.

Table I
PARAMETERS AND VALUES OF COMPONENTS.

Parameters	Symbols	Value
Grid voltage	vg	120–240 V
Output voltage	Vo	360 V
Grid frequency	fg	60 Hz
Switching frequency	fs	50 kHz
Rated output power	Po	1 kW
Primary capacitor	Cin	6.6 µF
Primary inductor	Lin	940 µH
Magnetizing inductance	Lm	300 µH
Primary leakage inductance	Llk,p	1.39 µH
Secondary leakage inductance	Llk,s	0.86 µH
Snubber capacitance	Csn1, Csn2	22 nF
Snubber resistance	Rsn1, Rsn2	200 kΩ
Resonant capacitance	Cr	4.4 µF
Output capacitance	Co	1320 µF

During CCM, ZCS turn-off is guaranteed at Diode D2. The input current was almost sinusoidal. Input current i_{in} was synchronized with vg and had measured PF = 0.9.
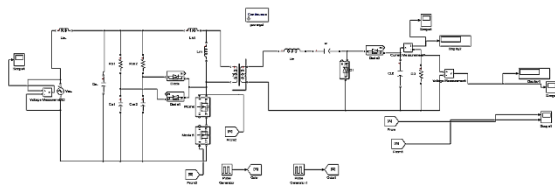
4.1 Open loop simulation of proposed converter

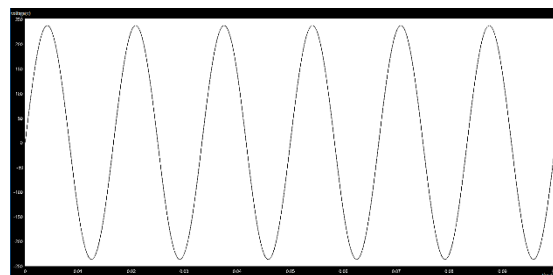**Fig. 4.1. Simulink model of open loop system.**

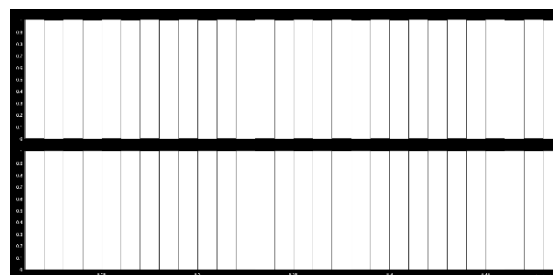**Fig. 4.2. Input voltage waveform.**

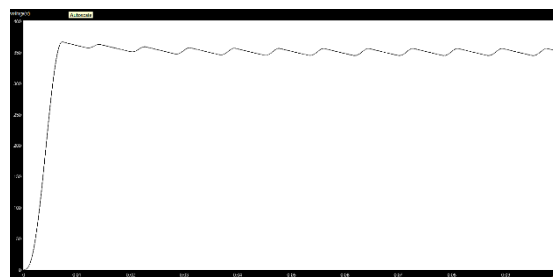**Fig. 4.3. Gate pulses to switch S1 and S2.**

Fig. 4.4. Output Voltage.

Fig. 4.5. Output current.

The output voltage equation is given by:

$$V_o = V_g n(D + 1) \quad (15)$$
$$V_o = 240 * 1 * (0.5 + 1)$$
$$V_o = 360\ V (\text{Theoritical value})$$

By simulation

$$V_o = 351\ V$$

The output voltage obtained in open loop simulation is Vo = 351 V. This discrepancy is because of the semiconductor devices (switch and diode) voltage drop when they are on.

Output power is given by:

$$Po = Vo * Io$$
$$P = 351*2.7$$
$$P = 947.7W$$

Power obtained in open loop simulation is 947.7W which is less than required value hence we go for closed loop circuit.

4.1.1 Closed loop simulation of proposed converter
4.1.1.1 Block diagram of converter with pi controller

The output of the converters is not constant because of the difference in the environmental condition therefore control techniques are employed. Hence to achieve the required output voltage to meet the load demand, closed loop control is implemented. The block diagram shown in figure 4.1.1 explains the implementation of proportional integral (pi) controller for single phase resonant ac-dc converter. The actual output voltage of the bridgeless resonant ac-dc converter and the constant reference signal are compared, to obtain a error signal. The error signal (e) is given to proportional integral (pi) controller. The pi controller generates the control signal based on error signal for varying the turn on and turn off time of the switch of the bridgeless resonant ac-dc converter, to maintain constant output voltage(Vo) irrespective of the load variation and input voltage. Similarly to maintain constant output current pi controller is used.

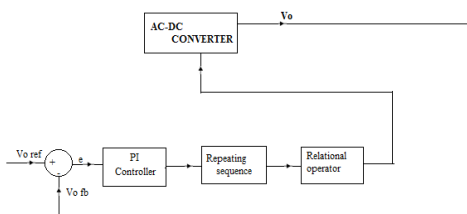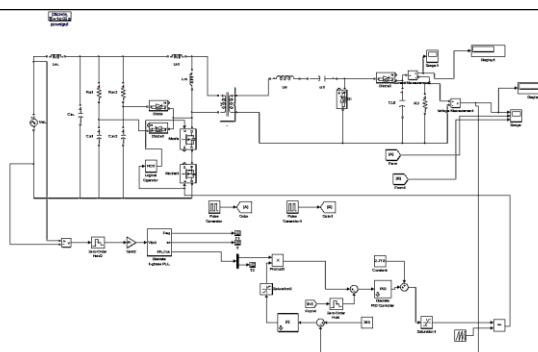**Fig. 4.1.1. Block diagram of resonant ac-dc converter.**

Fig. 4.1.2Simulink model of closed loop system.

Fig. 4.1.3 Output voltage in closed loop.

Fig. 4.1.4. Output current in closed loop.

By closed loop simulation
$$V_o = 360\ V$$
$$Po = Vo * Io$$
$$Po = 360*2.778$$
$$Po = 1KW$$

Power obtained in closed loop simulation with pi controller is 1KW which is the required power level.

Remark 1. The proposed converter operates similar to the forward converter andduring the half switching period it transfer the energy to the load in resonant way. Then,during other half switching period the proposed converter transfers the magnetizing energy in the transformer to the series resonant circuit.

Remark 2. The applications of the converter is common dc-bus supplier in the buildings/mobile charging stations. It can be also be used as level-2 battery charger by connecting the proposed converters in parallel. Furthermore, it can be used in high voltage applications such as traveling wave tube,medical X-ray imaging, and lasers.

V. CONCLUSION

This paper presents a bridgeless single phase resonant ac-dc converter. To reduce the number of components, the grid-side full-bridge diode rectifier is replaced by a single bidirectional switch; as a result, the primary side conduction lossand number of components were both reduced. Use of a series-resonant voltage-doubler structure reduced the cost and size of the proposed converter and enables its use in medium-high power applications.Moreover the proposed converter

achieves accurate output voltage regulation and high PF. To confirm the validity of the proposed converter, open loop and closed loop simulation was performed.

REFERENCES

[1]. 80 Plus Incentive Program. [Online]. Available: http://www.80plus.org

[2]. M. Narimani and G. Moschopoulos, "A new interleaved threephase single-stage PFC AC–DC converter with flying capacitor," *IEEE Trans. Power Electron.,* vol. 30, no. 7, pp. 3695-3702, Jul. 2015.

[3]. B. Poorali and E. Adib, "Analysis of the integrated SEPICflyback converter as a single-stage single-switch power-factorcorrection LED driver," *IEEE Trans. Ind. Electron.,* vol. 63, no. 6, pp. 3562-3570, Jun. 2016.

[4]. H. Ma, J. S. J. Lai, C. Zheng, and P. Sun, "A high-efficiency quasi-single-stage bridgeless electrolytic capacitor-free highpower AC–DC driver for supplying multiple LED strings in parallel," *IEEE Trans. Power Electron.*, vol. 31, no. 8, pp. 58255836, Aug. 2016.

[5]. P.FangandY.F.Liu,"EnergychannelingLEDd rivertechnology to achieve flicker-free operation With true single stage power factor correction," *IEEE Trans. Power Electron.,* vol. 32, no. 5, pp. 3892-3907, May 2017.

[6]. S. Li, W. Qi, S. C. Tan, and S. R. Hui, "A single-stage two-switch PFC rectifier with automatic AC ripple power decoupling and wide output voltage range," *IEEE Trans. Power Electron.*, vol. 32, no. 9, pp. 6971-6982, Sep. 2017.

[7]. S. Li, W. Qi, S. C. Tan, and S. R. Hui, "A single-stage two-switch PFC rectifier with wide output voltage range and automatic AC ripple power decoupling," *IEEE Trans. Power Electron.*, vol. 32, no. 9, pp. 6971-6982, Sep. 2017.

[8]. Y. W. Cho, J. M. Kwon, and B. H. Kwon, "Single powerconversion AC–DC converter with high power factor and high efficiency," *IEEE Trans. Power Electron.*, vol. 29, no. 9, pp. 4797-4806, Sep. 2014.

[9]. S. G. Jeong, W. J. Cha, S. H. Lee, J. M. Kwon, and B. H. Kwon, "Electrolytic capacitor-less single-power-conversion onboard charger with high efficiency," *IEEE Trans. Ind. Electron.,* vol. 63, no. 12, pp. 7488-7497, Dec. 2016.

[10]. K. S. Kim, J. M. Kwon, and B. H. Kwon, "Single-switch single power-conversion PFC converter using regenerative snubber," *IEEE Trans. Ind. Electron.,* vol. 65, no. 7, pp. 5436-5444, Jul. 2018.

[11]. L. Huber, Y. Jang, and M. M. Jovanovic, "Performance evaluation of bridgeless PFC boost rectifiers," *IEEE Trans. Power Electron.,* vol. 23, no. 3, pp. 1381-1390, Mar. 2008.

[12]. B. Su, J. Zhang, and Z. Lu, "Totem-pole boost bridgeless PFC rectifier with simple zero-current detection and full-range ZVS operating at the boundary of DCM/CCM," *IEEE Trans. Power Electron.,* vol. 26, no. 2, pp. 427-435, Feb. 2011.

[13]. W. Y. Choi and J. S. Yoo, "A bridgeless single-stage half-bridge AC/DC converter," *IEEE Trans. Power Electron.*, vol. 26, no. 12, pp. 3884-3895, Dec. 2011.

[14]. S. W. Lee and H. L. Do, "Single-stage bridgeless ac–dc PFC converter using a lossless passive snubber and valley switching," *IEEE Trans. Ind. Electron.,* vol. 63, no. 10, pp. 6055-6063, Oct. 2016.

[15]. M. Alam, W. Eberle, D. S. Gautam, C. Botting, N. Dohmeier, and F. Musavi, "A hybrid resonant pulse-width modulation bridgeless AC–DC power factor correction converter," *IEEE Trans. Ind. Appl.,* vol. 53, no. 2, pp. 1406-1415, Feb. 2017.

[16]. A. Malschitzky, F. Albuquerque, E. Agostini, and C. B. Nascimento, "Single-stage integrated bridgeless-boost nonresonant half-bridge converter for LED driver applications," *IEEE Trans. Ind. Electron.,* vol. 65, no. 5, pp. 3866-3878, May 2018.

[17]. H. Ma, Y. Li, J. S. Lai, C. Zheng, and J. Xu, "An improved bridgeless SEPIC converter without circulating losses and input voltage sensing," *IEEE Trans. Emerg. Sel. Topics Power Electron.,* vol. 6, no. 3, pp. 1447 - 1455, Sep. 2018.

[18]. J. W. Shin, S. J. Choi, and B. H. Cho, "High-efficiency bridgeless flyback rectifier with bidirectional switch and dual output windings," *IEEE Trans. Power Electron.,* vol. 29, no. 9, pp. 4752-4762, Sep. 2014.

[19]. E. H. Kim and B. H. Kwon, "Zero-voltage- and zero-currentswitching full-bridge converter with secondary resonance," *IEEE Trans. Ind. Electron.,* vol. 57, no. 3, pp. 1017-1025, Mar. 2010.